Inhibitory effect of antibodies against the cell adhesion molecule gicerin on gastric cancer progression

SAAYA UENO, NAO UEMURA, KAZUHIDE ADACHI and YASUHIRO TSUKAMOTO

Laboratory of Animal Hygiene, Department of Agricultural and Life Science, Faculty of Life and Environmental Sciences, Kyoto Prefectural University, Kyoto 606-8522, Japan

Received April 29, 2025; Accepted August 29, 2025

DOI: 10.3892/mmr.2025.13687

Abstract. Gicerin is a member of the immunoglobulin superfamily, which functions as a cell adhesion molecule that is expressed in developing and regenerating tissues, as well as in various types of tumors. In malignant neoplasms, gicerin has been implicated in promoting cellular invasion and metastasis. The present study aimed to investigate whether or not anti-gicerin antibodies could inhibit the progression of the human gastric cancer cell line NUGC-4 in a murine model. First, immunofluorescence staining was employed to confirm gicerin expression in the NUGC-4 cells. The cells were subsequently pretreated with either anti-gicerin antibodies or pre-immune IgG and transplanted subcutaneously into nude mice, where the extent of tumor growth and local invasion were both assessed. In a separate hematogenous metastasis model, mice received a tail-vein injection of NUGC-4 cells pretreated in an identical manner and pulmonary metastases were evaluated. Anti-gicerin antibody pretreatment led to a significant suppression of subcutaneous tumor formation, histological invasiveness and lung nodule formation compared with the controls. Taken together, these findings suggested that the antibody-mediated inhibition of gicerin reduced both local tumor progression and hematogenous spread in gastric cancer, highlighting gicerin as a promising therapeutic target that potentially may be effective when used in combination with conventional chemotherapy.

Introduction

Cell adhesion molecules fulfill critical roles in embryonic development, tissue repair and intercellular communication (1,2). In cancer, dynamic regulation of adhesion and detachment underlies tumor invasion and metastasis (3). The progression and metastasis of cancer are coordinated by intricate molecular mechanisms that transcend mere tumor cell proliferation, encompassing dynamic interactions with the surrounding tumor microenvironment. Among these mechanisms, cell adhesion molecules (CAMs) have emerged as pivotal regulators of malignant behaviors, including cancer cell adhesion, migration and invasion and also interaction with the vascular endothelium, thereby facilitating metastatic dissemination and the acquisition of aggressive phenotypes (4,5). Major CAM families, including cadherins, integrins, selectins and members of the immunoglobulin superfamily, contribute to tumor progression through distinct, yet often interrelated, signaling pathways. For example, the loss of E-cadherin expression is a well-established trigger of epithelial-mesenchymal transition, promoting the enhanced motility, invasiveness and metastatic potential of cancer cells (6). Integrins, which mediate cell-extracellular matrix interactions, exert critical roles in cellular migration and angiogenesis. Alterations in the expression of specific integrin subunits have previously been associated with unfavorable clinical outcomes in various malignancies (7). Moreover, accumulating evidence has shown that CAMs function not only as structural mediators, but also as active transducers of intracellular signaling cascades that regulate tumor cell survival, therapeutic resistance and immune evasion (8). In particular, studies have highlighted that alterations in the expression and function of CAMs are closely associated with the progression of gastric cancer (9-14). Dysregulated CAM expression, such as reduced E-cadherin or aberrant integrin profiles, has been linked to enhanced tumor invasiveness, lymph node metastasis and poor clinical prognosis in patients with gastric carcinoma (2,3,6-8,11). These findings suggest that CAMs play a critical role not only in early tumor development but also in the acquisition of metastatic traits in gastric cancer. The present study focused on a specific CAM, gicerin, that has been implicated in gastric cancer progression. Through an analysis of its expression profile and functional roles, the aim of this study was to elucidate its potential as a novel therapeutic target in gastric cancer treatment.

Gicerin, originally identified from chicken gizzard smooth muscle, shares high homology with mammalian CD146/MelCAM (15-19). As described in more detail below, it has five immunoglobulin-like domains in its extracellular

Correspondence to: Professor Yasuhiro Tsukamoto, Laboratory of Animal Hygiene, Department of Agricultural and Life Science, Faculty of Life and Environmental Sciences, Kyoto Prefectural University, 1-5 Nakaragi-cho, Shimogamo, Sakyo-ku, Kyoto 606-8522, Japan
E-mail: ytsuka@kpu.ac.jp

Key words: gicerin, cell adhesion molecule, antibody, gastric cancer cells, metastasis

region and two major isoforms [long (L)-gicerin and short (S)-gicerin)] have been shown to be generated by alternative splicing (19-22). Gicerin is a single-pass transmembrane glycoprotein localized to the cell membrane and comprises a large extracellular domain, a single transmembrane segment and a short cytoplasmic domain. The extracellular region contains five immunoglobulin-like loop structures, two of the V-set type and three of the C2-set type, as well as several potential N-linked glycosylation sites. The cytoplasmic domain is predicted to contain four serine/threonine phosphorylation sites, suggesting that gicerin may be involved in cell adhesion and intracellular signal transduction.

Gicerin has been shown to engage in both homophilic and heterophilic interactions, including those with specific laminins, influencing processes such as cell migration and neurite extension (19,20). Although it is widely expressed during embryogenesis, gicerin is limited in normal adult tissues to sites such as vascular endothelium and muscle (19,20). However, re-expression of gicerin in malignant tumors has been shown to be associated with enhanced invasiveness and metastatic potential (15,19,20).

Gastric cancer is a common gastrointestinal malignancy, frequently metastasizing to the liver and peritoneum, with occasional, but significant, pulmonary metastases (23-25). Studies have indicated that various cell adhesion molecules are critical regulators of metastasis in gastric cancer, highlighting them as potential therapeutic targets (9-14,26,27). Cell adhesion molecules, such as E-cadherin, claudin, contactin 1, mucin 1 and L1 cell adhesion molecule, are known to facilitate or inhibit tumor progression and gicerin is likely to have a comparable role in gastric cancer.

NUGC-4, a poorly differentiated gastric adenocarcinoma cell line, is commonly used for *in vivo* modeling of tumor growth and metastasis (28). In the present study, it was shown that NUGC-4 cells expressed gicerin and the study also evaluated how anti-gicerin antibodies affect their subcutaneous tumorigenicity and lung metastatic potential in nude mice.

Materials and methods

Immunization and purification of anti-gicerin antibodies. To generate polyclonal antibodies against gicerin, 10 female BALB/c mice (6-8 weeks old) were immunized with recombinant gicerin protein. The primary immunization was performed subcutaneously with 50 μg of recombinant rat gicerin protein (aa 1-545; accession number Q9EPF2-1) (29), which exhibits ~70% peptide-sequence homology to the human gicerin ortholog, emulsified in an equal volume of Complete Freund's Adjuvant (MilliporeSigma). Booster injections were administered on days 14 and 28 using an identical dose of antigen emulsified in Incomplete Freund's Adjuvant (MilliporeSigma). On day 42, mice were deeply anesthetized using isoflurane (induction at 3-5% and maintenance at 2-3% in oxygen) and the absence of reflex responses (pedal withdrawal and palpebral reflexes) was confirmed before proceeding. For terminal blood collection, cardiac puncture was performed under deep anesthesia using a 1 ml syringe with a 23-gauge needle. Blood (~0.5-1.0 ml) was withdrawn from the left ventricle. Following the procedure, sacrifice of the mice was performed by cervical dislocation while under deep anesthesia, or alternatively by thoracotomy to confirm the cessation of cardiac activity. Finally, mortality was verified by the absence of a heartbeat and fixed, dilated pupils. All animal procedures were conducted in accordance with institutional guidelines and were approved by the Animal Care and Use Committee of Kyoto Prefecture University (approval no. KPU240401). A total of 55 mice, including those reserved as backups, were used for antibody production and tumor cell transplantation in the present study.

Collected blood samples were allowed to clot at room temperature for 1 h prior to centrifugation at 1,500 x g for 10 min at 4˚C to isolate serum. The sera from all mice were pooled and total IgG was purified using a Protein G Sepharose column (GE Healthcare) following the manufacturer's protocol. Bound IgG was eluted with 0.1 M glycine-HCl buffer (pH 2.7) and immediately neutralized with 1 M Tris-HCl (pH 9.0). The eluates were subsequently dialyzed against phosphate-buffered saline (PBS) (pH 7.4) and the IgG concentrations were determined spectrophotometrically. Similarly, serum was collected from non-immunized normal mice and IgG was purified using protein G affinity chromatography. The resulting antibodies were used as pre-immune IgG.

For the isolation of gicerin-specific antibodies, affinity purification was performed using a custom-made column prepared by covalently coupling recombinant gicerin protein to CNBr-activated Sepharose 4B beads (Cytiva). The purified IgG was subsequently loaded onto the affinity column equilibrated with PBS. After extensive washing, bound antibodies were eluted with 0.1 M glycine-HCl buffer (pH 2.7) and immediately neutralized, as aforementioned. The eluted antibodies were then dialyzed against PBS and protein concentrations were quantified using a BCA Protein Assay Kit (Thermo Fisher Scientific, Inc.). The final purified anti-gicerin antibodies were subsequently adjusted to a concentration of 1 mg/ml in PBS and stored at -80˚C until use. The overview of antibody production and purification is shown in Fig. 1A.

Sodium dodecyl sulfate-polyacrylamide gel electrophoresis (SDS-PAGE) and Coomassie Brilliant Blue (CBB) Staining. Recombinant gicerin protein and mouse antibodies were separated by SDS-PAGE on 8% gels. Protein samples were mixed with Laemmli sample buffer, heated at 95˚C for 5 min and loaded onto an 8% polyacrylamide gel. Electrophoresis was carried out under reducing conditions using a Mini-PROTEAN Tetra System (Bio-Rad Laboratories, Inc.) at a constant voltage of 100 V. After electrophoresis, the gel was briefly rinsed with distilled water and stained using Coomassie Brilliant Blue R-250 staining solution (Bio-Rad Laboratories, Inc.) for 1 h at room temperature. The gel was subsequently destained with a solution containing 40% methanol and 10% acetic acid until protein bands became clearly visible.

Enzyme linked immunosorbent assay (ELISA). Each well of the polystyrene ELISA plates (Sumitomo Bakelite Co., Ltd.) was coated with 0.2 μg of recombinant gicerin proteins in PBS and the plate was incubated over night at 4˚C. Each of the following incubation steps were preceded by washing the wells twice with PBS containing 0.05% Tween 20. The wells were blocked for nonspecific binding by the addition of a commercial blocking buffer (DS Pharma Biomedical Co., Ltd.) and were

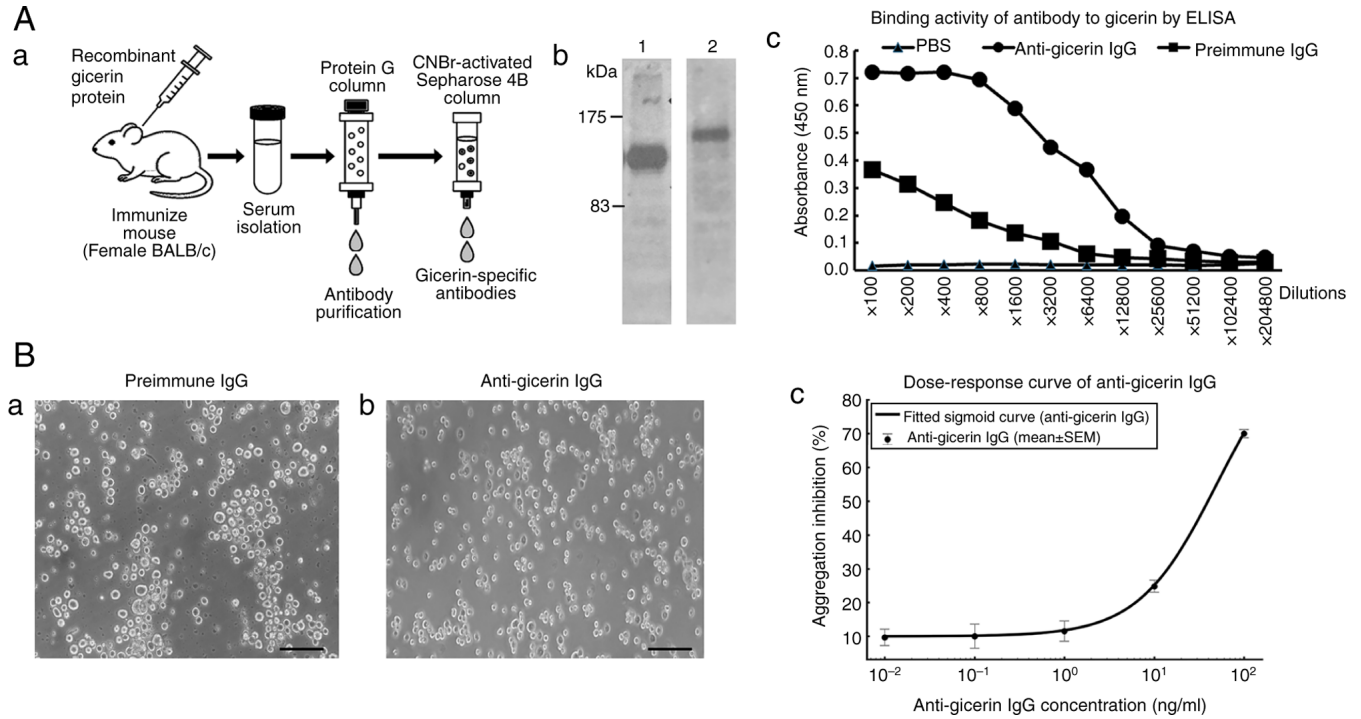

Figure 1. Generation of mouse anti-gicerin antibody and validation of its binding activity. (A) The procedure for generating and purifying the murine anti-gicerin antibody is summarized. (a) BALB/c mice were immunized with recombinant gicerin protein, followed by IgG purification from serum. The IgG fraction was subsequently affinity-purified using a Sepharose column conjugated with gicerin protein. (b) As shown by SDS-PAGE, the gicerin recombinant protein immunized as the antigen for antibody production (lane 1) appeared as a single band at ~120 kDa, while the final purified mouse IgG (lane 2) exhibited a single band at ~150 kDa. Binding activity of mouse IgG to gicerin proteins by ELISA. (c) Recombinant proteins of gicerin were bound to plate at 2 μg/ml overnight at 4˚C. Samples were blocked with 1% blocking buffer (Block Ace) in distilled water for 2 h. Serial dilutions of pre-immune or anti-gicerin IgG were incubated at room temperature for 2 h. After washing with PBS, HRP-conjugated polyclonal antibody against mouse IgGs were reacted for 1 h at room temperature. Then, 3,3',5,5'-tetramethylbenzidine was added to each well and plates were read at 450 nm utilizing a Multiscan JX (Thermo Fisher Scientific, Inc.). ELISA demonstrated that the purified antibody exhibited strong binding activity to gicerin protein, with an ELISA titer of 12,800 when compared to pre-immune IgG. (B) Neutralizing activity of anti-gicerin IgG in cell adhesion. (a) In the cell aggregation assay, L-929 cells expressing gicerin formed multicellular aggregates upon the addition of pre-immune IgG, indicating cell-cell adhesion. (b) When the anti-gicerin IgG was added to the suspension cultures, a marked inhibition of cell-cell aggregation was observed. Scale bars, 100 μm; magnification, x200. (c) Dose-response curves were generated by plotting the aggregation index against the logarithmic antibody concentrations. Nonlinear regression analysis determined that the IC_{50} of anti-gicerin IgG was 49.5 ng/ml, indicating its potent neutralizing effect on cell adhesion. IC_{50}, half-maximal inhibitory concentration.

incubated at 37˚C for 2 h. The serial dilutions of pre-immune IgG and anti-gicerin IgG were added vertically to the wells and kept for incubation at 37˚C for 1 h. The HRP-conjugated rabbit IgG diluted (1:5,000) in PBS was dispensed into each well. The plate was incubated for 1 h at 37˚C. Later, a substrate buffer containing TMB (Sumitomo Bakelite Co., Ltd.) was added to each well and kept for incubation at 37˚C for 15 min. The reaction was terminated by the addition of a stopping reagent (1.25M sulfuric acid). The absorbance was recorded at 450 nm using the ELISA plate reader (DS Pharma Biomedical Co., Ltd.). The ELISA titer was defined as the highest dilution factor of anti-gicerin IgG that yielded an absorbance value at least three times higher than that obtained with pre-immune IgG.

Neutralization activity of anti-gicerin IgG on cell-cell interactions. Reaggregation assay and determination of IC_{50} for anti-gicerin antibody: A reaggregation assay was performed to evaluate the inhibitory effect of anti-gicerin mouse IgG on cell-cell adhesion in gicerin transfected L929 cells (RIKEN BioResource Research Center; cat. no. RCB2619) (30). The cells were cultured in Dulbecco's Modified Eagle Medium (DMEM; high glucose) supplemented with L-glutamine, sodium pyruvate, 10% fetal bovine serum (FBS) and antibiotics (Nacalai Tesque, Inc.) and maintained at 37˚C in a humidified atmosphere containing 5% CO_2. Then, the cells were detached using 0.02% EDTA in calcium- and magnesium-free PBS to obtain a single-cell suspension. The cells were then washed twice with calcium- and magnesium-containing Hank's Balanced Salt Solution (HBSS) and resuspended at a concentration of $1x10^6$ cells/ml. Serial dilutions of purified anti-gicerin mouse IgG (0, 0.01, 0.1, 1, 10 and 100 ng/ml) or control non-immune mouse IgG were prepared in HBSS. Equal volumes of antibody solution and cell suspension were mixed and transferred to 96-well U-bottom low-adhesion plates (100 μl/well). The mixtures were incubated at 37˚C for 30 min to allow antibody binding. Subsequently, the plate was gently agitated on an orbital shaker (50 rpm) and incubated for an additional 45 min at 37˚C to promote cell-cell reaggregation. Following incubation, the degree of cell aggregation in each well was assessed by phase-contrast microscopy. A cell aggregate composed of at least four cells was counted as a single unit for analysis (21). Images of representative fields (five per well) were captured at x200 magnification. Aggregation was quantified by calculating the inhibition of cell aggregation (%), defined as

follows: Inhibition of cell aggregation (%)=100 x (1-number of single cells/total number of cells).

Cell line and culture conditions. NUGC-4 cells (JCRB Cell Bank; cat no. JCRB0834), HUVEC cells [JCRB Cell Bank; cat. no. IFO50271; F10 (passage 10)] and murine melanoma B16 cells (RIKEN BioResource Research Center; cat. no. RCB1283) were cultured in DMEM (high glucose) supplemented with L-glutamine, sodium pyruvate, 10% FBS and antibiotics (Nacalai Tesque, Inc.) and maintained at 37˚C in a humidified atmosphere containing 5% CO_2.

Confirmation of gicerin expression on NUGC-4 cells and HUVECs. Monolayers of NUGC-4 and HUVEC cells were fixed using Zamboni's fixative and incubated with a murine polyclonal anti-gicerin antibody (1:500; generated as aforementioned) at 37˚C, followed by an FITC-conjugated goat anti-mouse IgG (1:100; MilliporeSigma; cat. no. AP124F) at 37˚C. In addition, tumor tissues harvested from mice were fixed in Zamboni's solution and frozen sections (20 μm thickness) were subjected to immunofluorescence staining using the anti-gicerin primary antibody followed by the FITC-conjugated secondary antibody as aforementioned. Fluorescence microscopy revealed the distinct membrane-localized expression of gicerin on cells. A commercially available mounting medium containing DAPI was employed following the manufacturer's instructions. While nuclear staining was achieved, the combined display of phase-contrast, FITC (gicerin) and DAPI slightly reduced the clarity of cell contours in our setup; therefore, the final images are presented without DAPI to best illustrate the relationship between cell morphology and gicerin expression in the same field of view.

Protein extraction and western blot analysis. Cultured NUGC-4, HUVEC and B16 cells were rinsed twice with calcium- and magnesium-free Hanks' balanced salt solution and collected using a cell scraper. The harvested monolayer cells were subsequently homogenized in PBS using a Polytron homogenizer. The homogenates were centrifuged at 1,000 x g for 10 min at 4˚C to remove cellular debris, followed by centrifugation of the supernatants at 18,000 x g for 30 min at 4˚C. The resulting pellets were resuspended in 10 mM Tris-acetate buffer (pH 8.0) containing 1 mM EDTA and 0.5% Nonidet P-40 and incubated at 4˚C for 1 h with continuous rotation. The suspensions were subsequently centrifuged at 40,000 x g for 90 min at 4˚C and the final supernatants were collected for western blot analysis, as described by Taniura *et al* (31). Protein concentrations were quantified using BCA Protein Assay Reagent (Pierce; Thermo Fisher Scientific, Inc.) at an absorbance of 562 nm, with bovine serum albumin as a standard. Equal amounts of total protein (20 μg) extracted from HUVEC, NUGC-4 and B16 cells, along with 10 ng recombinant gicerin protein and mouse IgG, were separated by SDS-PAGE using 7.5% polyacrylamide gels and electrotransferred on to polyvinylidene difluoride (PVDF) membranes (Bio-Rad Laboratories, Inc.). The membranes were blocked with Bullet Blocking One reagent (Nacalai Tesque, Inc.; cat. no. 1379) and subsequently incubated for 1 h at room temperature with primary anti-gicerin antibodies which were generated as aforementioned) diluted 1:1,000 in 2% skimmed milk in Tris-buffered saline (TBS) buffer (150 mM NaCl/10 mM Tris-HCl, pH 8.0). After six washes with TBST buffer (TBS buffer containing 0.05% Tween-20), the membranes were incubated for 1 h at room temperature with horseradish peroxidase-conjugated goat anti-rabbit IgG (Nacalai Tesque, Inc.; cat. no. 21860-61l) diluted 1:1,000 in TBS buffer containing 2% skimmed milk. Following four washes with TBST and two final washes with TBS, immunoreactive bands were visualized using 0.05% diaminobenzidine (MilliporeSigma) in 50 mM Tris-HCl (pH 7.6) containing 0.03% hydrogen peroxide for 5 min at room temperature. The reaction was stopped by rinsing in distilled water. Images of the membranes were captured using a ChemiDoc imaging system (Bio-Rad Laboratories, Inc.) as previously described (19,20).

Subcutaneous tumor transplantation model. Subcutaneous implantation of tumor cells into the cervical region of nude mice offers several advantages (32). The cervical area provides a soft and accessible site that facilitates precise and reproducible injection of the cell suspension, minimizing procedural variability. Tumors formed in this region tend to grow outward beneath the skin, allowing for easy visual assessment and accurate measurement of tumor size using calipers. Additionally, the relatively stable blood supply in the cervical skin reduces the risk of ulceration, thereby enabling long-term observation and reliable evaluation of therapeutic efficacy. Since the tumor remains localized in the cervical area, vital organs such as those of the gastrointestinal and urinary systems are less likely to be affected, contributing to the maintenance of the general condition of the animals and allowing for consistent assessment of drug effects and toxicity. Moreover, because cervical tumors rarely interfere with the mobility or feeding behavior of the animals, this model supports the ethical conduct of experiments while minimizing distress to the animals. After harvesting the NUGC-4 cells with trypsin-EDTA (Nacalai Tesque, Inc.), the cells were split into two groups. One group was incubated with anti-gicerin IgG (10 μg/ml), whereas the other was incubated with pre-immune IgG (10 μg/ml) for 1 h at 37˚C. Cells were washed and resuspended in serum-free DMEM ($3x10^7$ cells/ml) and 0.2 ml cell suspension was injected subcutaneously into the dorsal cervical region of nude mice (9-week-old female BALB/c Slc-nu/nu mice; n=5 per group). Tumor volume was calculated every other day starting at 1-week post-inoculation using the formula $(AxB^2)/2$, where A and B represent the largest and smallest tumor diameters, respectively.

After the final measurement, mice were deeply anesthetized using isoflurane (induction at 3-5% and maintenance at 2-3% in oxygen) and the absence of reflex responses (pedal withdrawal and palpebral reflexes) was confirmed before proceeding with the experiment. Sacrifice was performed by cervical dislocation while the mice were in a state of deep anesthesia, or alternatively by thoracotomy to confirm the cessation of cardiac activity. Mortality was verified by the absence of a heartbeat and fixed, dilated pupils. In accordance with institutional animal care guidelines, the maximum allowable tumor volume was limited to 1.5 cm^3. Mice were sacrificed immediately upon reaching this limit or upon exhibiting signs of pain, ulceration or impaired mobility; however, no animals exhibited such conditions during the course of the experiment.

Pathologically, the tumors were excised, 10% buffered-formalin-fixed for 48 h at room temperature, paraffin-embedded and stained with hematoxylin for 5 min at room temperature (22-25˚C), followed by eosin staining for 3 min at room temperature [hematoxylin and eosin (H&E) staining] for a histopathological assessment of local invasion. For immunofluorescence staining, tumor tissues were fixed in Zamboni's fixative, followed by cryoprotection in 20% sucrose solution for 24 h at 4˚C. The samples were subsequently frozen at -30˚C and 20-μm frozen sections were prepared using a cryostat. The frozen sections were blocked with 1% non-fat dry milk in PBS containing 0.1% Tween-20 for 1 h at room temperature, and were subsequently incubated with a murine polyclonal anti-gicerin antibody (1:500; generated as aforementioned) at 37˚C, followed by an FITC-conjugated goat anti-mouse IgG (1:100; MilliporeSigma; cat. no. AP124F) at 37˚C as aforementioned. Fluorescence microscopy revealed the distinct membrane-localized expression of gicerin on cells.

Hematogenous pulmonary metastasis model. NUGC-4 cells ($2.5x10^6$ cells/ml) were pretreated with anti-gicerin antibodies or pre-immune IgG under the same conditions. Each mouse (n=5 per group) received a 0.1 ml tail-vein injection of either of the treated cell suspensions. After 1 week, mice were sacrificed and lungs were collected, formalin-fixed, paraffin-embedded and stained with H&E, as aforementioned. The number of metastatic foci was counted in all lung lobes and expressed as nodules per cm^2. In these experiments, mice were deeply anesthetized using isoflurane (induction at 3-5% and maintenance at 2-3% in oxygen) and the absence of reflex responses (pedal withdrawal and palpebral reflexes) was confirmed prior to the performance of any procedure. Sacrifice was performed as aforementioned and mortality was verified by the absence of a heartbeat and the presence of fixed, dilated pupils. In cases where mice exhibited clinical signs such as respiratory distress or lethargy, sacrifice was to have been performed immediately to minimize suffering; however, no animals exhibited such symptoms during the course of the experiment.

In vitro cell adhesion of NUGC-4 cells to gicerin proteins: Cell adhesion experiments were carried out as reported previously (21). Aliquots (1 ml) of PBS containing 10ng/ml of recombinant gicerin proteins were spotted on a 35 mm culture dish and incubated for 1 h in a humidified 5% CO_2 in incubator at 37˚C. Then the dishes were washed with DMEM three times and preincubated with DMEM containing 10% FBS for 1 h to block nonspecific binding. Aliquots (2 ml) of the cell suspension ($1x10^6$ cells/ml) were plated on the test dishes. To assess the inhibition of adhesion activity by anti-gicerin antibody, the cells were preincubated for 30 min at 37˚C with the pre-immune IgG or anti-gicerin IgG at a final concentration of 100 ng/ml before plating on the dishes. The test dishes were incubated for 1 h at 37˚C, washed twice with DMEM and the adhesion cells were observed by phase-contrast microscopy.

In vitro cell adhesion of NUGC-4 cells to vascular endothelial cells. Endogenous gicerin-positive HUVEC cells, a vascular endothelial cell line, were cultured on dishes with DMEM containing 10% FBS at 37˚C and used as feeder layers. The NUGC-4 cell suspensions were preincubated with anti-gicerin polyclonal antibodies or pre-immune IgG for 1 h at 37˚C. After five washing in PBS and centrifugation at 800 x g for 10 min at 4˚C, the NUGC-4 cells were resuspended in DMEM and seeded on to the HUVEC monolayers. Following a 30 min incubation at 37˚C, the cultures were gently washed with DMEM and removed and the NUGC-4 cells adhering to the feeder layers were observed under a light microscope (Nikon Corporation). The cell number per area was determined for five areas and the average scores and standard deviation (SD) were calculated.

Measurement of doubling time of NUGC-4 cells with antibodies. NUGC-4 cells were seeded into 6-well tissue culture plates at a density of $2x10^4$ cells per well in complete DMEM supplemented with 10% FBS. The cells were incubated at 37˚C in a humidified atmosphere containing 5% CO_2. After 4 h to allow for cell attachment, 10 μl of phosphate-buffered saline (PBS), 10 μl of pre-immune IgG, or 10 μl (10 ng/ml) of anti-gicerin IgG (10 ng/ml) was added to each well, respectively. For each treatment group, a total of four independent plates (n=4) were prepared and analyzed. At 0, 24, 48 and 72 h after seeding, one well from each plate was harvested. Cells were gently washed with PBS, detached using 0.25% trypsin-EDTA and resuspended in culture medium. Cell viability was assessed using trypan blue exclusion and viable cells were counted with a hemocytometer. Only unstained (viable) cells were included in the count.

Doubling time (T_d) was calculated using the following formula:

$$T_d = \frac{t \cdot \log(2)}{\log(N_t/N_0)}$$

where t is the elapsed time (in h), N_0 is the number of viable cells at time 0 and Nt is the number of viable cells at time t. The mean doubling time were calculated for each treatment group. Statistical comparison was performed between the pre-immune IgG group and anti-gicerin IgG using Student's t-test.

In vitro cell migration assay. NUGC-4 cells on culture dishes coated with gicerin protein (as aforementioned) were cultured in DMEM supplemented with 10% FBS at 37˚C in a humidified atmosphere containing 5% CO_2 until they reached confluence. A straight scratch was made across the center of each well using a sterile yellow 200-μl micropipette tip to detach cells along the line. The medium was carefully aspirated to remove the detached cells and replaced with fresh serum-free DMEM. The cells were then treated with either pre-immune IgG (100 ng/ml) or anti-gicerin IgG (100 ng/ml) and incubated under the same conditions. Cell migration into the scratched area was monitored daily under a light microscope for up to 96 h.

Complement-dependent cytotoxicity (CDC) assay. NUGC-4 cells were cultured in DMEM supplemented with 10% FBS and seeded into 24-well culture plates (Corning, Inc.). Cells were subsequently incubated at 37˚C in a humidified atmosphere containing 5% CO_2 until they reached semi-confluence. After removal of the culture medium, cells were gently rinsed with PBS. Subsequently, serum-free DMEM containing either pre-immune IgG or anti-gicerin polyclonal antibody

was added to each well. The final antibody concentration was adjusted to 10 μg/ml. Cells were incubated at 37˚C for 1 h. Following antibody treatment, cells were washed gently two or three times with PBS to remove any unbound antibodies. Fresh mouse serum (complement-active) or heat-inactivated mouse serum (treated at 56˚C for 30 min) was subsequently diluted in serum-free DMEM to a final concentration of 20% and added to the cells. After a 1 h incubation at 37˚C, the supernatant containing non-adherent cells was collected and temporarily maintained at 37˚C, while the adherent cells were detached using trypsin-EDTA. The cell suspension and supernatant were mixed in the tubes and subsequently centrifuged at 300 x g for 5 min. The pellet was then resuspended in either PBS or serum-free DMEM. Cell viability was subsequently assessed using the trypan blue exclusion method. Equal volumes of cell suspension and 0.4% trypan blue solution were mixed and the mixture was loaded onto a hemocytometer. Viable (unstained) and non-viable (blue-stained) cells were counted under a light microscope and the cell death rate (as a percentage) was calculated using the following formula: Cell death rate (%)=number of blue-stained cells/total number of cells x100. At least five independent wells were analyzed per treatment group.

Statistical analysis. All quantitative data are presented as mean ± standard deviation (SD). For *in vivo* experiments, n=5 mice per group; for *in vitro* assays, at least n=4 independent replicates per group unless otherwise indicated. Two-tailed, unpaired Student's t-tests were used for single pairwise comparisons and one-way analysis of variance (ANOVA) followed by Tukey's honestly significant difference (HSD) test was used for ≥3-group comparisons. Exact P-values are reported on the graphs and/or in the figure legends; where thresholds are shown, significance is denoted as $^{*}P<0.05$, $^{**}P<0.01$ and $^{*}P<0.001$; 'ns' indicates $P\geq0.05$. Error bars on all graphs represent SD and all '±' values denote SD. $P<0.05$ was considered to indicate a statistically significant difference.

Results

Generation and purification of murine anti-gicerin antibody. The procedure for generating and purifying the murine anti-gicerin antibody is summarized in Fig. 1A. BALB/c mice were immunized with recombinant gicerin protein, followed by IgG purification from serum. The IgG fraction was subsequently affinity-purified using a Sepharose column conjugated with gicerin protein. SDS-PAGE analysis revealed a single band at ~150 kDa in the final purified fraction, indicating that a highly pure IgG preparation was obtained. Furthermore, ELISA demonstrated that the purified antibody exhibited strong binding activity to gicerin protein, with an ELISA titer of 12,800 when compared to pre-immune IgG.

Neutralizing activity of anti-gicerin IgG in cell adhesion. The neutralizing activity of anti-gicerin IgG was evaluated using a cell aggregation assay. When anti-gicerin IgG was added to the suspension culture of gicerin-expressing L929 cells, a marked inhibition of cell-cell aggregation was observed (Fig. 1Ba and Bb). Dose-response curves were generated by plotting the aggregation index against the logarithmic antibody concentrations (Fig. 1Bc). Nonlinear regression analysis determined that the half-maximal inhibitory concentration (IC_{50}) of anti-gicerin IgG was 49.5 ng/ml, indicating its potent neutralizing effect on cell adhesion.

Gicerin is expressed in NUGC-4 cells. Immunofluorescence analysis revealed the presence of distinct membrane-associated signals in NUGC-4 cells, confirming robust gicerin expression (Fig. 2A). As a limitation of this study, it was unable to perform co-localization staining with another inner membrane protein. This was due to the poor adherence of NUGC-4 cells, which made them susceptible to detachment during the multiple steps required for double immunofluorescence staining, such as repeated washing, antibody incubation and prolonged handling. Western blot analysis demonstrated that gicerin was expressed in the membrane fractions of B16 and HUVEC cells, both of which are known to endogenously express gicerin, similarly to the recombinant protein. In addition, gicerin expression was also detected in NUGC-4 cells (Fig. 2B). Notably, doublet bands were observed at ~120 kDa, indicating that NUGC-4 cells express both the S- and the L-isoforms of gicerin (19,20).

Subcutaneous tumor growth and invasion is reduced in the subcutaneous tumor model. In the subcutaneous tumor model, tumor masses derived from cells treated with anti-gicerin antibody exhibited markedly suppressed tumor growth compared with the control group ($P<0.01$; Fig. 3A). Immunofluorescence analysis further revealed strong gicerin expression on the membranes of tumor cells and in the endothelial cells of newly formed blood vessels within tumors located in the cervicodorsal region of the implanted mice (Fig. 3B). Moreover, histopathological analysis revealed that tumors in the control group exhibited extensive invasion into the dermis, muscle and adipose tissue. In addition, epithelial-like arrangements of tumor cells were observed in the control group, thereby revealing histological features consistent with poorly differentiated adenocarcinoma. By contrast, tumors in the anti-gicerin antibody-treated group were more circumscribed and exhibited markedly reduced local invasiveness. Furthermore, frequent and prominent focal necrotic lesions were observed in tumors from animals administered the anti-gicerin antibody. Within these tumors, cellular degeneration, structural disintegration, pyknosis and karyorrhexis were also frequently noted (Fig. 3C).

Pulmonary metastasis is suppressed in the tail-vein injection model. In the tail-vein injection model, mice that received pre-immune IgG-treated cells were found to develop multiple tumor nodules in the lung parenchyma, often accompanied by hemorrhagic changes (Fig. 4). By contrast, mice injected with anti-gicerin antibody-treated cells exhibited markedly fewer metastatic lesions, indicating substantial inhibition of hematogenous spread.

Inhibition of NUGC-4 cell adhesion to gicerin-coated surfaces by anti-gicerin antibody. To evaluate the role of gicerin in mediating cell adhesion, culture dishes were coated with recombinant gicerin protein and seeded with NUGC-4 cells. A substantial number of cells adhered to the gicerin-coated surface under control conditions. However, in the presence of

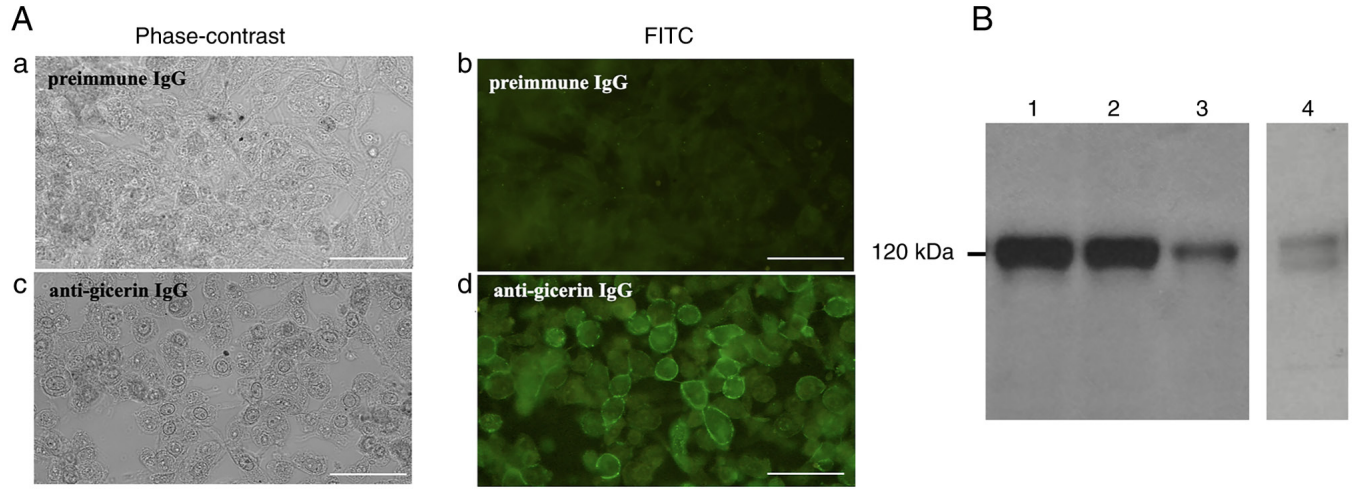

Figure 2. Gicerin expression in NUGC-4 cells. (A) Indirect immunofluorescence staining of NUGC-4 cells was performed and observed under a fluorescence microscope (as shown by the B-excitation filter). No fluorescence was detected when pre-immune IgG was applied (a, phase contrast; b, immunofluorescence). By contrast, strong green fluorescence was observed on the cell surface following staining with anti-gicerin IgG (c, phase contrast; d, immunofluorescence), indicating membrane-associated expression of gicerin. scale bars, 50 μm; magnification, x400. (B) Western blot analysis of membrane fractions from B16 (lane 2), HUVEC (lane 3) and NUGC-4 cells (lane 4) following SDS-PAGE. The recombinant gicerin protein used as the immunogen was also subjected to electrophoresis as a positive control and to verify the specificity and reactivity of the antibody (lane 1). Notably, a doublet band of ~120 kDa was observed in lane 4, consistent with the expression of both the short and long isoforms of gicerin in NUGC-4 cells.

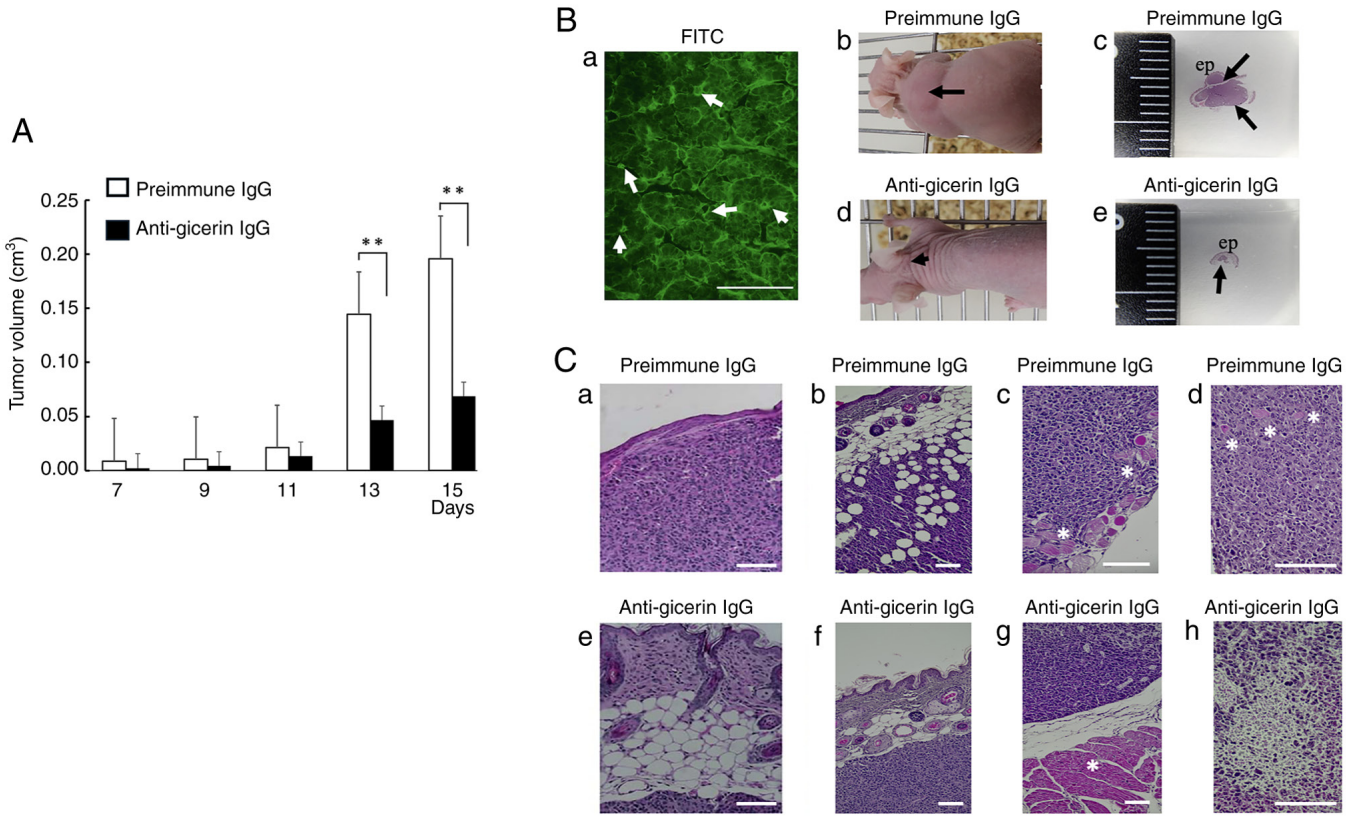

Figure 3. Tumor growth and histopathological features following subcutaneous injection into nude mice. (A) NUGC-4 cells treated with either pre-immune IgG or anti-gicerin IgG were subcutaneously injected into the dorsal neck region of nude mice (n=5 per group). Tumor volume was measured over time using the formula: $AxB^2/2$, where A and B represent the maximum and minimum tumor diameters, respectively. Data are mean ± SD (n=5 mice per group). Two-tailed unpaired Student's t-tests were performed between pre-immune IgG and anti-gicerin IgG at each time point. Significance indicators: ns ($P \geq 0.05$), $^{*}P<0.05$, $^{**}P<0.01$. (B) On day 15 post-injection, tumor tissues were examined both histologically and using immunofluorescence analysis. (a) Gicerin expression was detected in the tumor cell membranes, especially in epithelial-like structures, as well as in neovascular structures (denoted by the arrows) scale bars, 100 μm; magnification, x200. Compared with mice injected with pre-immune IgG (b and c), those injected with anti-gicerin IgG displayed smaller tumor masses and reduced tumor areas histologically with hematoxylin and eosin staining (arrows) (d and e). (C) In the pre-immune IgG group, histological evidence of tumor invasion into the dermis (a), adipose tissue (b), subcutaneous muscle (c) and undifferentiated adenocarcinoma (d) regions was noted (arrows indicate invasion into the muscle). (e-g) By contrast, mice treated with anti-gicerin IgG showed markedly reduced tumor invasiveness. (h) Furthermore, signs of cellular degeneration, structural disintegration, pyknosis and karyorrhexis were frequently observed within tumors treated with anti-gicerin antibody. Scale bars, 100 μm; magnification: a and e: x100; b, f and g: x50; and c, d and h, x200.

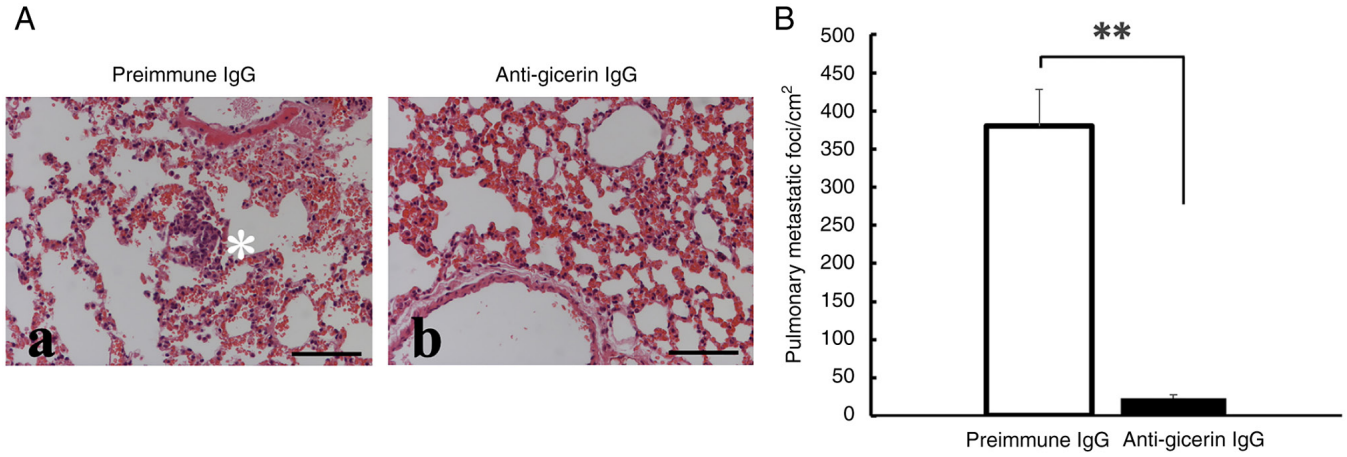

Figure 4. Pulmonary metastasis following tail vein injection in nude mice. (A) NUGC-4 cells pretreated with either pre-immune IgG or anti-gicerin IgG were injected into the tail veins of nude mice (n=5 per group). On day 15, lung tissues were harvested and examined histologically. (a) In the pre-immune IgG group, multiple metastatic foci were observed, characterized by epithelial-like tumor cell proliferation and frequent hemorrhaging. (b) By contrast, few metastatic lesions were detected in the anti-gicerin IgG group. Scale bar, 100 μm; magnification, x100. (B) The number of metastatic foci per unit area in lung tissue was quantified histologically. Data are shown as mean ± SD (n=5 mice per group). Between-group comparison was performed with a two-tailed unpaired Student's t-test; the difference was statistically significant. Significance indicators: ns ($P \geq 0.05$), $^{*}P<0.05$, $^{**}P<0.01$.

anti-gicerin antibody, cell adhesion to the gicerin-coated areas was markedly inhibited, as evidenced by a significant reduction in the number of adherent cells (Fig. 5A). These findings demonstrated that the anti-gicerin antibody effectively neutralizes the homophilic binding activity of gicerin, thereby suppressing gicerin-mediated adhesion of NUGC-4 cells.

In vitro cell adhesion of the NUGC-4 cells to vascular endothelial cells. When HUVECs were used as a feeder layer and NUGC-4 cells were seeded, a substantial number of NUGC-4 cells adhered to the surface of HUVECs. Immunofluorescence staining subsequently revealed that gicerin was positively expressed in the monolayer of HUVEC cells, as well as in the NUGC-4 cells adhering to them (Fig. 5B). In this experiment, two-color staining was attempted to visualize HUVECs, which served as the feeder layer and the NUGC-4 cells adhered to them. However, successful fluorescence-based visualization could not be achieved. The reason for this was that the adhesion of NUGC-4 cells to HUVECs was weak and during the double-staining procedure, where gicerin on HUVECs was labeled red with rhodamine and gicerin on NUGC-4 cells was labeled green using a FITC-conjugated antibody, the NUGC-4 cells detached. Therefore, it was not possible to perform dual staining with different dyes. In this condition, NUGC-4 cells adhered to the surface of HUVECs with a small, rounded morphology. Based on this morphology and the observed fluorescence, both NUGC-4 cells and HUVECs were confirmed to express gicerin, as evidenced by the green fluorescence emitted by both cell types. Notably, the fluorescence intensity was stronger in NUGC-4 cells. These findings clearly demonstrate gicerin positivity in both cell types through their morphological and fluorescence characteristics.

The addition of an anti-gicerin antibody markedly decreased the number of NUGC-4 cells that adhered to HUVECs compared with the addition of pre-immune IgG, demonstrating that the anti-gicerin antibody could inhibit the adhesion of NUGC-4 cells to vascular endothelial cells (Fig. 5C).

In vitro cell migration assay. To examine the involvement of gicerin in the migratory potential of NUGC-4 cells, an *in vitro* scratch assay were performed. Notably, NUGC-4 cells treated with pre-immune IgG exhibited markedly greater migration into the scratched area compared with those treated with anti-gicerin IgG (Fig. 5D). By day 4, the scratched area was completely closed in the pre-immune IgG group, whereas cell migration was markedly delayed in the group treated with anti-gicerin antibody. These findings suggested that gicerin expression facilitates the migration of NUGC-4 cells.

Measurement of cell death by CDC assay. When pre-immune IgG was used, the addition of fresh serum did not induce cell death. By contrast, significant levels of cell death were observed when fresh murine serum was added to NUGC-4 cells preincubated with anti-gicerin IgG; however, no cell death occurred when heat-inactivated serum was used (Fig. 6A). Taken together, these results suggested that complement activity in the serum, engaged by the anti-gicerin IgG bound to NUGC-4 cells, is responsible for inducing cell death (Fig. 6B). The doubling time of NUGC-4 cells was 23.4 h. When pre-immune IgG was added, the doubling time was 24.7 h and when anti-gicerin IgG was added, it was 22.5 h (Fig. 6C). These findings suggest that the addition of anti-gicerin IgG does not affect the proliferation of gastric cancer cells: no significant difference between pre-immune IgG and anti-gicerin IgG groups; ($P<0.05$).

Discussion

The present study demonstrated that gicerin was highly expressed in NUGC-4 gastric cancer cells and that the specific binding of these cells to anti-gicerin antibodies markedly suppressed subcutaneous tumor growth, local invasion and pulmonary metastasis in an *in vivo* model. These observations are all consistent with previous studies, which suggest that gicerin fulfills a critical role in tumor metastasis (16,19,20). Notably, the cell-adhesive properties of gicerin appear to enhance interactions between tumor cells and the surrounding

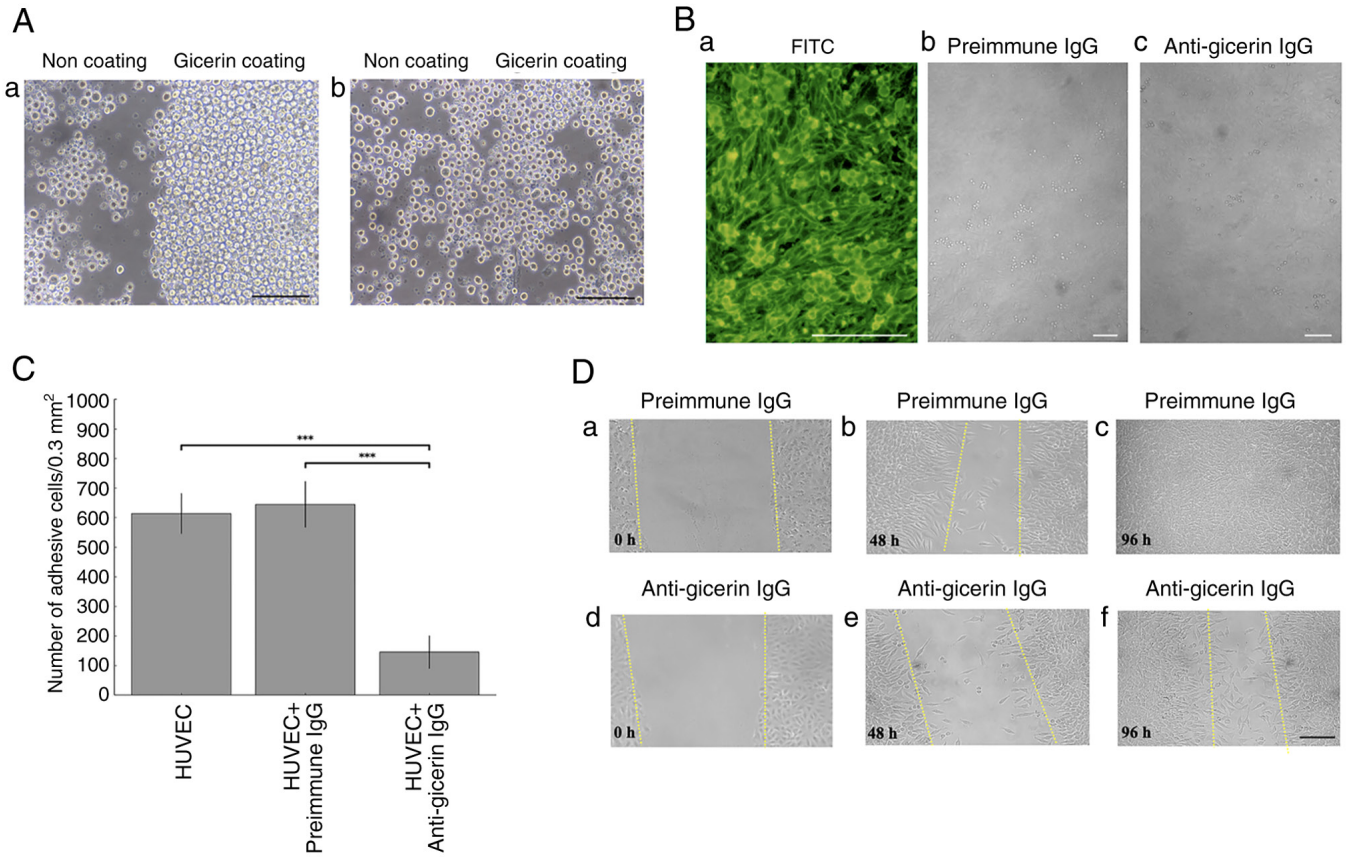

Figure 5. (A) Inhibition of NUGC-4 cell adhesion to gicerin protein by anti-gicerin antibody. Only the right half of each culture dish was coated with recombinant gicerin protein. NUGC-4 cell adhesion was assessed under a phase-contrast microscope. (a) The cells predominantly adhered to the gicerin-coated region, indicating that NUGC-4 cells exhibit homophilic binding through gicerin molecules expressed on their surface. Adhesion was not inhibited by pre-immune IgG. (b) By contrast, treatment with anti-gicerin IgG markedly suppressed the attachment of NUGC-4 cells to the gicerin-coated area. These findings demonstrate that anti-gicerin IgG effectively blocks the homophilic adhesion ability of NUGC-4 cells via gicerin. Scale bars, 100 μm; magnification x200. (B) Adhesion of NUGC-4 cells to HUVEC monolayers. (a) Immunofluorescence staining revealed gicerin expression on both adherent NUGC-4 cells and HUVEC feeder cells. NUGC-4 cells treated with either (b) pre-immune IgG or (c) anti-gicerin IgG were seeded on to confluent HUVEC monolayers. Compared with the pre-immune IgG group, the number of NUGC-4 cells attached to HUVEC layers was noticeably reduced in the anti-gicerin IgG group. Scale bar, 100 μm. Magnification: a, x200; and b and c, x50. (C) The number of NUGC-4 cells adhering to HUVECs was markedly lower in the anti-gicerin IgG group compared with the pre-immune control. Adherent cells were counted in randomly selected 0.3 mm^2 areas under light microscopy. Data are mean ± SD (n=5 independent replicates per group). Group differences were analyzed by one-way ANOVA followed by Tukey's HSD test across PBS, pre-immune IgG and anti-gicerin IgG conditions. Anti-gicerin IgG differed markedly from the other groups (***P<0.001), whereas other pairwise comparisons were not significant unless indicated. (D) Inhibition of NUGC-4 cell migration by anti-gicerin antibody. NUGC-4 cells were seeded on culture dishes pre-coated with gicerin protein and incubated until they reached confluence. (a) A linear scratch was made across the cell monolayer using the tip of a yellow pipette to create a cell-free area. (b) Culture media containing either pre-immune IgG or anti-gicerin IgG was then added and cell migration into the scratched area was monitored over time using phase-contrast microscopy. (b) In the presence of pre-immune IgG, numerous cells migrated into the scratch area by 48 h and (c) the wound was completely closed by 96 h. (d) By contrast, dishes treated with anti-gicerin IgG showed (e) markedly reduced cell migration at 48 h and (f) a large cell-free area remained even after 96 h. These findings indicate that anti-gicerin IgG inhibits gicerin-mediated cell motility. The dashed straight line indicates the edge of the wound at each time point after the initial scratch procedure. Scale bar, 100 μm; magnification: x100.

tissues (especially muscular and adipose tissues), as well as endothelial cells, thereby promoting the processes of intravasation, embolus formation and subsequent extravasation. Indeed, the findings in the present study have added further support to the hypothesis that gicerin facilitates *in vitro* adhesion of gastric cancer cells to endothelial cells. L-gicerin, which possesses a longer intracellular domain, has been shown to promote significant proliferative activity of the cells and metastasis to multiple organs, thereby driving tumor progression more effectively compared with S-gicerin, which has a shorter intracellular domain (20,26). Notably, the NUGC-4 cell line used in the present study expressed both gicerin isoforms. Although normal muscle tissue likewise expresses both isoforms, the biological significance of their co-expression remains poorly understood and elucidating the interplay between these two isoforms in NUGC-4 cells warrants further investigation.

Furthermore, the addition of anti-gicerin IgG to the culture medium was found not to alter the doubling time of tumor cells *in vitro*, suggesting that this antibody does not directly suppress tumor cell proliferation under these conditions. However, in the mouse subcutaneous tumor model, the presence of anti-gicerin IgG did markedly inhibit tumor growth, suggesting that antibody bound to the tumor surface may interact with factors in the tumor microenvironment, thereby contributing to tumor control *in vivo*. Since tumor progression and expansion often involve interactions between cell adhesion molecules on the tumor surface and normal tissues, this finding highlighted the potential role of gicerin as a molecular mediator in these processes. In addition, the

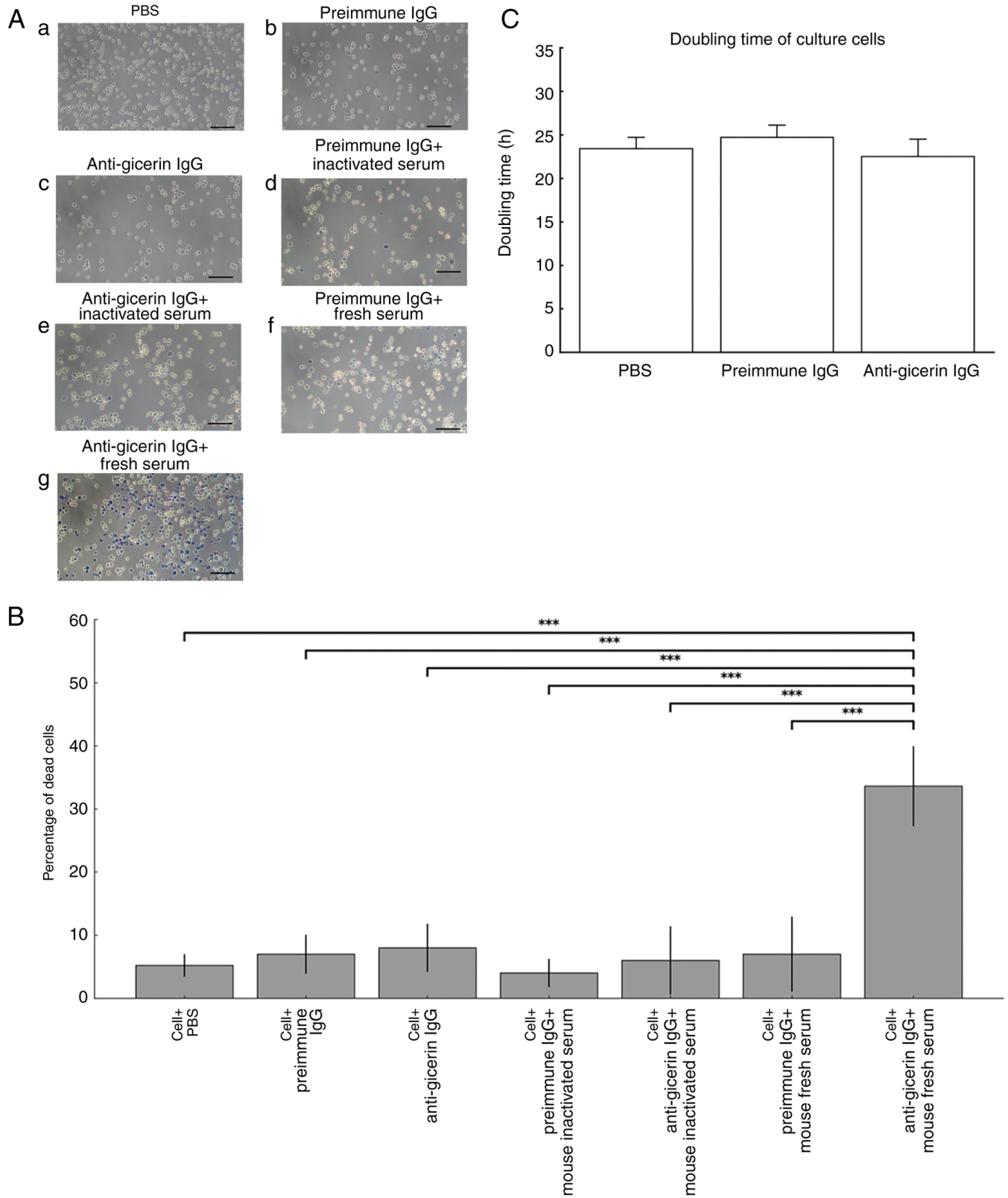

Figure 6. Complement-dependent cytotoxicity assay. (A) NUGC-4 cells were incubated with either pre-immune IgG or anti-gicerin IgG, followed by treatment with either fresh mouse serum (complement-active) or heat-inactivated serum (heated at 56˚C for 30 min). After a 1 h incubation at 37˚C, non-adherent cells were removed and adherent cells were detached by treating the cells with trypsin-EDTA. Cell viability was assessed using the trypan blue exclusion method under light microscopy (a, with PBS; b, with pre-immune IgG, c, with anti-gicerin IgG; d, with pre-immune IgG and inactivated serum; e, with anti-gicerin IgG and inactivated serum; f, pre-immune IgG and fresh serum; g, with anti-gicerin IgG and fresh serum. (B) Viable (unstained) and nonviable (blue-stained) cells were counted and the percentages of dead cells were calculated. Data are mean ± SD (n=5 independent replicates per group). Seven groups were compared by one-way ANOVA with Tukey's HSD; only the cell + anti-gicerin IgG + fresh mouse serum group differed markedly from all other groups ($^{***}P<0.001$). (C) Doubling times of NUGC-4 cells with anti-gicerin antibody. The cells were cultured with PBS, pre-immune IgG and anti-gicerin IgG and doubling times in each condition were calculated. As shown in the graph, anti-gicerin antibody did not affect the proliferation of NUGC-4 cells under *in vitro* conditions, similar to pre-immune IgG. Data are presented as mean ± SD (n=4 independent replicates per group). Differences among the three groups (PBS, pre-immune IgG and anti-gicerin IgG) were evaluated by one-way ANOVA followed by Tukey's HSD post hoc test; no statistically significant differences were detected.

in vitro data generated in the present study demonstrated that complement components in mouse blood can interact with anti-gicerin IgG to induce tumor cell death; hence, complement activation within the tumor milieu may further promote tumor cell destruction, ultimately reducing tumor growth, local infiltration and hematogenous metastasis to the lung. During tumorigenesis, cancer cells not only acquire the ability to evade host regulatory mechanisms, but also actively manipulate systemic homeostasis to favor their own survival and proliferation (33). Tumor-derived cytokines and hormones have been shown to influence key endocrine organs, including the hypothalamus, pituitary, adrenal glands and thyroid, thereby modulating central regulatory axes to establish a physiological milieu conducive to tumor growth and progression. It has been demonstrated that gicerin mediates homophilic interactions between gicerin molecules themselves, which facilitate the adhesion of tumor cells to each other, to vascular tissues and to muscular structures (16,19,20,34-36). In addition, heterophilic interactions between gicerin and extracellular matrix (ECM) components have been suggested to promote local tissue invasion by tumor cells. These findings collectively indicate that gicerin may play a multifaceted role in tumor progression through both structural and signaling mechanisms. Notably, previous analyses also suggests that gicerin expression within tumors may contribute to intratumoral angiogenesis, possibly through factors expressed by tumor cells themselves (16,19,20,36-39). These mechanisms are not unique to experimental tumor models but are highly relevant to human gastric cancer as well. The current study further expanded on this knowledge by using a mouse-derived anti-gicerin antibody to target gicerin expressed on tumor cells within a murine model of gastric cancer. Unlike our previous work, which employed rabbit-derived antibodies to study gicerin function in tumors of murine and avian origin (16,19,20,34-36), the present study represented the first attempt, to the best of the authors' knowledge, to directly target gicerin within a living mouse using a homologous (murine) antibody. Strikingly, systemic administration of the mouse-derived anti-gicerin antibody resulted in widespread necrotic foci within the tumor tissue. This observation suggested that the murine antibodies, by engaging with mouse complement proteins, may have efficiently induced complement-mediated cytotoxicity against gicerin-expressing gastric cancer cells. This is in contrast to our *in vitro* findings, where the same anti-gicerin antibody had no effect on the proliferation rate (doubling time) of gastric cancer cells. Thus, the induction of tumor necrosis *in vivo* appears to be mediated by immune components present in the host, rather than by direct effects of the antibody on cell proliferation. In addition to directly inducing necrosis of the tumor itself, the mouse-derived anti-gicerin antibody may have disrupted gicerin-positive neovasculature within the tumor, thereby creating a hypoxic and energy-deficient microenvironment that led to secondary tumor cell necrosis. Furthermore, it remains an important issue for future investigation whether the suppression of gastric cancer progression by the antibody also involves the induction of apoptosis in cancer cells.

Additionally, the present study demonstrated that the antibody markedly suppressed the motility of gastric cancer cells cultured on gicerin-coated dishes. These findings support the hypothesis that gicerin plays a critical role in facilitating tumor cell migration and tissue infiltration, particularly in gastric cancer. In subsequent studies, it is planned to further dissect the interaction between gicerin and other adhesion molecules such as cadherins and vimentin, using *in vitro* chemotaxis systems and cell motility analyses in the presence of anti-gicerin antibodies.

The present study chose recombinant rat gicerin as the immunogen for antibody production. This decision was based on previous success in establishing a high-purity, large-scale production system for recombinant rat gicerin protein, which enabled the generation of highly sensitive neutralizing antibodies when used to immunize rabbit (29). By contrast, our attempts to produce recombinant human gicerin in large quantities were unsuccessful, as the yield from cultured cells was extremely low and insufficient for immunization. Given these technical constraints and the sufficient cross-reactivity of rat gicerin with human gicerin expressed on NUGC-4 gastric cancer cells, the present study opted to use recombinant rat gicerin to immunize mice, resulting in the successful generation of anti-gicerin IgG with potent neutralizing activity. Inhibitory anti gicerin monoclonal antibodies (such as AA98) bind the D4-D5 junction, stabilize the monomeric form and thereby suppress dimerization dependent signaling and cell migration (40). These functional surfaces (loops on D1 and D4-D5) are structurally conserved among mammals. The antibody in the present study was murine polyclonal, so it probably contained multiple IgG species that collectively recognize several conserved epitopes on human gicerin, which is consistent with the broad neutralization observed in adhesion/invasion/metastasis assays. The antibodies in the present study were not raised against a short peptide. Instead, it immunized with a purified recombinant rat gicerin soluble extracellular domain encompassing all five Ig like domains. The resulting product is a mouse polyclonal IgG (anti gicerin IgG) purified to high homogeneity. As the immunogen was the full ectodomain, the antibody preparation necessarily recognizing multiple linear and conformational epitopes distributed across the extracellular domains. Therefore, there is no single 'epitope location' or 'peptide sequence' applicable to this polyclonal.

Despite overall 70-72% identity between rat and human gicerin/CD146 in the extracellular region, functionally important surfaces within the Ig like domains are conserved. Prior structural work shows that inhibitory anti gicerin monoclonal antibodies (mAbs) can bind the D4-D5 interface and attenuate dimerization/activation. It is hypothesized that our polyclonal anti rat gicerin IgG contains subpopulations recognizing such conserved epitopes on human gicerin, which explained the neutralization of adhesion/invasion/metastasis observed in NUGC 4 cells. The present study did not perform epitope mapping. As follow up, it is planned to i) test binding to isolated human gicerin domain fragments (D1-D5), ii) run peptide competition or Pepscan ELISAs focusing on conserved surface loops within D1 and D4-D5 and iii) evaluate blocking against a reference inhibitory anti gicerin/CD146 mAb (e.g., AA98) to determine overlap. These experiments will pinpoint the dominant neutralizing epitopes.

In the development of antibody-based therapies, these results underscore the dual role of gicerin in gastric cancer:

not only as a structural adhesion molecule that facilitates tumor dissemination, but also as an immunological target whose inhibition may trigger tumor necrosis through host immune mechanisms. These findings collectively highlighted gicerin as a promising therapeutic target for the treatment of gastric cancer.

Nevertheless, further studies are warranted, both to clarify whether anti-gicerin antibodies primarily interfere with homophilic or with heterophilic binding and to elucidate the functions of distinct isoforms, if any should exist. Additional investigations focusing on established tumors and the possible synergistic effects of anti-gicerin therapy in combination with standard chemotherapy will be essential in order to define the clinical applicability of this strategy. Overall, these findings have strongly supported the potential usefulness of gicerin as a molecular target in the treatment of gastric cancer.

Gastric cancer cells actively shape their tumor microenvironment (TME) through several mechanisms that promote tumor survival, invasion and metastasis (41). First, gastric cancer cells secrete a range of cytokines and growth factors, such as VEGF, IL-6 and TGF-β, that modulate angiogenesis, stromal remodeling and immune cell recruitment. These factors contribute to the creation of a pro-tumorigenic environment by promoting vascularization, suppressing immune surveillance and enabling ECM degradation. Secondly, studies have shown that gastric cancer cells can induce polarization of tumor-associated macrophages toward an M2-like phenotype, which in turn supports tumor progression by secreting anti-inflammatory cytokines and matrix-remodeling enzymes. In addition, cancer-associated fibroblasts, often activated by tumor-derived signals, secrete ECM components and metalloproteinases that facilitate tumor cell migration and local invasion (4,33,41). Importantly, the present study suggested that the cell adhesion molecule gicerin may also participate in regulating the TME of gastric cancer. Gicerin-mediated interactions between tumor cells and endothelial or stromal cells may facilitate intravasation and immune evasion. Moreover, the observed complement-dependent cytotoxicity induced by anti-gicerin antibodies *in vivo* implied that gastric cancer cells may exploit gicerin to avoid complement activation under normal conditions, thereby maintaining TME homeostasis favorable to tumor growth.

However, when administering anti-gicerin antibodies to tumor-bearing animals, it is necessary to pretreat the antibody so as to minimize complement activation in the circulation. This cautionary measure arises from the fact that normal vascular and muscular tissues constitutively express gicerin; specifically, inadvertent binding of the antibody, followed by complement activation, could have deleterious effects on healthy tissues. Indeed, our preliminary pilot investigations revealed that the intravenous administration of intact anti-gicerin IgG to healthy mice induced pulmonary edema as a serious adverse event. Accordingly, before proceeding with *in vivo* therapeutic evaluations, there is a need to optimize the antibody protein to circumvent complement-mediated toxicity, which will thereby enhance the safety profile of this promising therapeutic strategy.

Collectively, the observed suppression of gastric cancer progression *in vivo* by the antibody may be attributed to the complement-mediated cytotoxic effect induced by anti-gicerin antibody in mice, as well as the inhibition of hematogenous metastasis and local tissue invasion through suppression of cell adhesion between gastric cancer cells and vascular endothelium. Cadherins are known to strengthen intercellular adhesion and their loss or mutation is associated with increased cancer cell invasion and metastasis. By contrast, cell adhesion molecules belonging to the immunoglobulin superfamily, such as gicerin, may play an opposing role. These findings support the concept that, *in vivo*, tumor progression is finely regulated by a complex network of multiple adhesion molecules and related factors.

Acknowledgements

Not applicable.

Funding

No funding was received.

Availability of data and materials

The data generated in the present study may be requested from the corresponding author.

Authors' contributions

SU was responsible for conceptualization of the project, performing the investigation, data analysis, writing and reviewing the manuscript and editing. NU was responsible for devising the methodology and validation of the data. KA performed the animal experiments. YT was responsible for conceptualization of the project, project administration, the acquisition of funding and preparation of the original draft of the manuscript. SU and YT confirm the authenticity of all the raw data. All authors read and approved the final manuscript.

Ethics approval and consent to participate

The use of HUVECs in this study was approved by the institutional review committee of Kyoto Prefectural University (Kyoto, Japan) at the time of cell purchase (approval no. OSP20190889). All animal experiments conducted in this study were reviewed for their scientific rationale and ethical justification and were approved by the Animal Experiment Committee of Kyoto Prefectural University (approval no. KPU240401). The authors declare that the animal experiment in this study was reviewed and approved by the institutional ethics committee without the participation of the project leader or any of the applicants in the review and approval process.

Patient consent for publication

Not applicable.

Competing interests

The authors declare they have no competing interests.

References

1. Cunningham BA: Cell adhesion molecules and signal transduction. Curr Opin Cell Biol 7: 628-633, 1995.
2. Albelda SM: Role of integrins and other cell adhesion molecules in tumor progression and metastasis. Lab Invest 68: 4-17, 1993.
3. Takeichi M: Cadherins in cancer: Implications for invasion and metastasis. Curr Opin Cell Biol 5: 806-811, 1993.
4. Hanahan D and Weinberg RA: Hallmarks of cancer: The next generation. Cell 144: 646-674, 2011.
5. Janiszewska M, Primi MC and Izard T: Cell adhesion in cancer: Beyond the migration of single cells. J Biol Chem 295: 2495-2505, 2020.
6. Berx G and van Roy F: The E-cadherin/catenin complex: An important gatekeeper in breast cancer tumorigenesis and malignant progression. Breast Cancer Res 3: 289-293, 2001.
7. Desgrosellier JS and Cheresh DA: Integrins in cancer: Biological implications and therapeutic opportunities. Nat Rev Cancer 10: 9-22, 2010.
8. Rathinam R and Alahari SK: Important role of integrins in the cancer biology. Cancer Metastasis Rev 29: 223-237, 2010.
9. Jung H, Jun KH, Jung JH, Chin HM and Park WB: The expression of claudin-1, claudin-2, claudin-3, and claudin-4 in gastric cancer tissue. J Surg Res 167: e185-e191, 2011.
10. Chen DL, Zeng ZL, Yang J, Ren C, Wang DS, Wu WJ and Xu RH: L1cam promotes tumor progression and metastasis and is an independent unfavorable prognostic factor in gastric cancer. J Hematol Oncol 6: 43, 2013.
11. Lu G, Cai Z, Jiang R, Tong F, Tu J, Chen Y, Fu Y, Sun J and Zhang T: Reduced expression of E-cadherin correlates with poor prognosis and unfavorable clinicopathological features in gastric carcinoma: A meta-analysis. Aging (Albany NY) 16: 10271-10298, 2024.
12. Gu L, Chen M, Guo D, Zhu H, Zhang W, Pan J, Zhong X, Li X, Qian H and Wang X: PD-L1 and gastric cancer prognosis: A systematic review and meta-analysis. PLoS One 12: e0182692, 2017.
13. Chen DH, Yu JW and Jiang BJ: Contactin 1: A potential therapeutic target and biomarker in gastric cancer. World J Gastroenterol 21: 9707-9716, 2015.
14. Singh P, Toom S and Huang Y: Anti-claudin 18.2 antibody as new targeted therapy for advanced gastric cancer. J Hematol Oncol 10: 105, 2017.
15. Tsukamoto Y, Taira E, Kotani T, Yamate J, Wada S, Takaha N, Miki N and Sakuma S: Involvement of gicerin, a cell adhesion molecule, in tracheal development and regeneration. Cell Growth Differ 7: 1761-1767, 1996.
16. Adachi K, Hattori M, Kato H, Inai M, Tsukamoto M, Handharyani E, Taira E and Tsukamoto Y: Involvement of gicerin, a cell adhesion molecule, in the portal metastasis of rat colorectal adenocarcinoma cells. Oncol Rep 24: 1427-1431, 2010.
17. Tsukamoto Y, Matsumoto T, Kotani T, Taira E, Takaha N, Miki N, Yamate J and Sakuma S: The expression of gicerin, a cell adhesion molecule, in regenerating process of collecting ducts and ureters of the chicken kidney after the nephrotrophic strain of infectious bronchitis virus infection. Avian Pathol 26: 245-255, 1997.
18. Tsukamoto Y, Taira E, Yamate J, Nakane Y, Kajimura K, Tsudzuki M, Kiso Y, Kotani T, Miki N and Sakuma S: Gicerin, a cell adhesion molecule, participates in the histogenesis of retina. J Neurobiol 33: 769-780, 1997.
19. Tsukamoto Y, Sakaiuchi T, Hiroi S, Furuya M, Tsuchiya S, Sasaki F, Miki N and Taira E: Expression of gicerin enhances the invasive and metastatic activities of a mouse mammary carcinoma cell line. Int J Oncol 23: 1671-1677, 2003.
20. Tsukamoto Y, Egawa M, Hiroi S, Furuya M, Tsuchiya S, Sasaki F, Miki N and Taira E: Gicerin, an Ig-superfamily cell adhesion molecule, promotes the invasive and metastatic activities of a mouse fibroblast cell line. J Cell Physiol 197: 103-109, 2003.
21. Taira E, Takaha N, Taniura H, Kim CH and Miki N: Molecular cloning and functional expression of gicerin, a novel cell adhesion molecule that binds to neurite outgrowth factor. Neuron 12: 861-872, 1994.
22. Taira E, Nagino T, Taniura H, Takaha N, Kim CH, Kuo CH, Li BS, Higuchi H and Miki N: Expression and functional analysis of a novel isoform of gicerin, an immunoglobulin superfamily cell adhesion molecule. J Biol Chem 270: 28681-28687, 1995.
23. Kong JH, Lee J, Yi CA, Park SH, Park JO, Park YS, Lim HY, Park KW and Kang WK: Lung metastases in metastatic gastric cancer: Pattern of lung metastases and clinical outcome. Gastric Cancer 15: 292-298, 2012.
24. Niimi T, Samejima J, Koike Y, Miyoshi T, Tane K, Aokage K, Taki T, Ishii G and Tsuboi M: A case of lung metastasis from gastric cancer presenting as ground-glass opacity dominant nodules. J Cardiothorac Surg 19: 365, 2024.
25. Chen ZR, Yang MF, Xie ZY, Wang PA, Zhang L, Huang ZH and Luo Y: Risk stratification in gastric cancer lung metastasis: Utilizing an overall survival nomogram and comparing it with previous staging. World J Gastrointest Surg 16: 357-381, 2024.
26. Rabben HL, Kodama Y, Nakamura M, Bones AM, Wang TC, Chen D, Zhao CM and Øverby A: Chemopreventive effects of dietary isothiocyanates in animal models of gastric cancer and synergistic anticancer effects with cisplatin in human gastric cancer cells. Front Pharmacol 12: 613458, 2021.
27. Li W, Zhao X, Wang H, Liu X, Zhao X, Huang M, Qiu L, Zhang W, Chen Z, Guo W, *et al*: Maintenance treatment of Uracil and Tegafur (UFT) in responders following first-line fluorouracil-based chemotherapy in metastatic gastric cancer: A randomized phase II study. Oncotarget 8: 37826-37834, 2017.
28. Akiyama S, Amo H, Watanabe T, Matsuyama M, Sakamoto J, Imaizumi M, Ichihashi H, Kondo T and Takagi H: Characteristics of three human gastric cancer cell lines, NU-GC-2, NU-GC-3 and NU-GC-4. Jpn J Surg 18: 438-446, 1988.
29. Taira E, Kohama K, Tsukamoto Y, Okumura S and Miki N: Characterization of Gicerin/MUC18/CD146 in the rat nervous system. J Cell Physiol 198: 377-387, 2004.
30. Taira E, Nagino T, Tsukamoto Y, Okumura S, Muraoka O, Sasaki F and Miki N: Cytoplasmic domain is not essential for the cell adhesion activities of gicerin, an Ig-superfamily molecule. Exp Cell Res 253: 697-703, 1999.
31. Taniura H, Kuo CH, Hayashi Y and Miki N: Purification and characterization of an 82-kD membrane protein as a neurite outgrowth factor binding protein: Possible involvement of NOF binding protein in axonal outgrowth in developing retina. J Cell Biol 112: 313-322, 1991.
32. Spyridopoulou K, Aindelis G, Lampri E, Giorgalli M, Lamprianidou E, Kotsianidis I, Tsingotjidou A, Pappa A, Kalogirou O and Chlichlia K: Improving the subcutaneous mouse tumor model by effective manipulation of magnetic nanoparticles-treated implanted cancer cells. Ann Biomed Eng 46: 1975-1987, 2018.
33. Slominski RM, Raman C, Chen JY and Slominski AT: How cancer hijacks the body's homeostasis through the neuroendocrine system. Trends Neurosci 46: 263-275, 2023.
34. Tsukamoto Y, Taira E, Miki N and Sasaki F: The role of gicerin, a novel cell adhesion molecule, in development, regeneration and neoplasia. Histol Histopathol 16: 563-571, 2001.
35. Tsuchiya S, Tsukamoto Y, Furuya M, Hiroi S, Miki N, Sasaki F and Taira E: Gicerin, a cell adhesion molecule, promotes the metastasis of lymphoma cells of the chicken. Cell Tissue Res 314: 389-397, 2003.
36. Kirimura N, Kubota Y, Adachi K and Tsukamoto Y: Involvement of gicerin, a cell adhesion molecule, in the hematogenous metastatic activities of a melanoma cell line. Am Int J Biol 2: 65-75, 2014.
37. Kohama K, Tsukamoto Y, Fruya M, Okamura K, Tanaka H, Miki N and Taira E: Molecular cloning and analysis of the mouse gicerin gene. Neurochem Int 46: 465-470, 2005.
38. Taira E, Kohama K, Tsukamoto Y, Okumura S and Miki N. Gicerin/CD146 is involved in neurite extension of NGF-treated PC12 cells. J Cell physiol 204: 632-637, 2005.
39. Tsuchiya S, Tsukamoto Y, Taira E and LaMarre J: Involvement of transforming growth factor-beta in the expression of gicerin, a cell adhesion molecule, in the regeneration of hepatocytes. Int J Mol Med 19: 381-386, 2007.
40. Chen X, Yan H, Liu D, Xu Q, Duan H, Feng J, Yan X and Xie C: Structure basis for AA98 inhibition on the activation of endothelial cells mediated by CD146. iScience 24: 102417, 2021.
41. Matsuoka T and Masakazu Y: Molecular mechanism for malignant progression of gastric cancer within the tumor microenvironment. Int J Mol Sci 25: 11735, 2024.